



Effect of bioceramic powder abrasion on different implant surfaces

Eman Abuhajar BDS, MSc (Clin), PhD¹ | Nesreen A. Salim BDS, MSc, PhD²  |
 Julian D. Satterthwaite BDS, MSc, PhD³ | Nick Silikas BSc (Hons), MPhil, PhD, FADM⁴ |
 Lamya M. Anweigi BDS, MMedSc, MFDS, PhD⁵ 

¹Faculty of Medicine, Dentistry and Oral Surgery, University of Tripoli, Tripoli, Libya

²Prosthetic Department, School of Dentistry, The University of Jordan, Consultant in Fixed and Removable Prosthodontics, The University of Jordan Hospital, Amman, Jordan

³Division of Dentistry, School of Medical Sciences, The University of Manchester, Manchester, UK

⁴School of Dentistry, The University of Manchester, Manchester, UK

⁵College of Dental Medicine, QU Health, Qatar University, Doha, Qatar

Correspondence

Lamya M. Anweigi, BDS, MMedSc, MFDS, PhD, College of Dental Medicine, Qatar University, Doha, Qatar.
 Email: lanweigi@qu.edu.qa

Abstract

Purpose: Bioceramic coatings have been shown to promote bone repair, which aids in the early integration of implants. This study aimed to evaluate the influence of air abrasion with a bioceramic abrasive on the surface characteristics of different implant materials and surfaces. The dissolution of the applied treatment from the surfaces over 3 weeks was also assessed.

Materials and Methods: Discs of three alloys used for dental implants were studied and compared: two types of commercially pure titanium (CpTi)/ (CpTi SLActive) and titanium-zirconia (TiZr). The tested surfaces were: CpTi control (CpC), sandblasted (SB), sandblasted and acid-etched (SBE), and CpTi SLActive®, (TiZr) Roxolid®. Three discs from each group underwent air abrasion with apatite bioceramic powders, 95% hydroxyapatite (HA)/5% calcium oxide (CaO), and 90% hydroxyapatite (HA)/10% calcium oxide (CaO). The treated discs were surface characterized by optical profilometry to obtain surface roughness, scanning electron microscopy (SEM), and energy dispersive X-ray spectroscopy (EDS) to compare element weight percentages of titanium, calcium, and phosphate. Dissolution was assessed using inductively coupled plasma optic emission spectrometry (ICP-OES).

Results: Bioceramic powders were deposited on all tested surfaces leading to changes in surface characteristics. The only statistically significant differences between the material groups for surface roughness were found with 95% HA/5% CaO powder in the Sp and Rp parameters ($p = 0.03$ and 0.04 , respectively). There were no significant differences in the Ca and P wt% between all groups and powders 95% HA/5% CaO and 90% HA/10% CaO ($p = 0.14$, 0.18 , and $p = 0.15$, 0.12 , respectively). A non-uniform dispersion of the treatment on the surface layer was visible on all treated surfaces. The bioceramic powder continued to dissolve from the tested surfaces for 3 weeks.

Conclusion: Bioceramic abrasion modifies implant surface characteristics, although the change in surface characteristics resulting from such treatment was not influenced by the implant material or surface treatment. Air abrasion with hydroxyapatite and calcium oxide bioceramics leaves powder deposits on the treated implant surfaces that could potentially influence the healing of implants affected by peri-implantitis.

KEYWORDS

air abrasion, bioceramic, calcium oxide, dental implants, hydroxyapatite, peri-implantitis, surface treatment

This is an open access article under the terms of the [Creative Commons Attribution](https://creativecommons.org/licenses/by/4.0/) License, which permits use, distribution and reproduction in any medium, provided the original work is properly cited.

© 2024 The Authors. *Journal of Prosthodontics* published by Wiley Periodicals LLC on behalf of American College of Prosthodontists.

Endosseous dental implants are frequently utilized as one of the treatment methods to restore lost teeth.^{1,2} Dental implants have good long-term survival and are highly predictable.² Replacement of missing teeth with implants is predicted to rise as a result of an increase in life expectancy, necessitating further developments to maintain the stability and functionality of dental implants over the long term.³

Osseointegration was defined by Albrektsson and Zarb as the method of maintaining an alloplastic dental implant in the host bone asymptotically throughout functional loading.⁴ One of the six crucial elements for effective anchoring of a dental implant in the host bone is the implant surface.⁵ The implant surface has a major impact on the early stage of osteoblast cell response and influences how well the implant integrates into the surrounding bone tissues.⁶ It has been demonstrated that rougher implant surfaces significantly aid in the process of the osseointegration of dental implants into the bone, thus enhancements to implant surface design such as creating a moderately roughened surface aim to boost success rates further or enabling the placed implants to be loaded sooner.^{7,8}

A further approach to altering implant surfaces relates to coating the surface. It has been demonstrated that implant coatings made of hydroxyapatite (HA) and other bioceramic materials can induce osteogenesis at the host-implant contact by releasing calcium phosphate ions. Due to the existence of these mineral components in natural bone, calcium, and phosphorus-based compounds have been specifically added as coating materials for dental implants.⁷ After implantation, the release of calcium phosphate from the surface coating saturates nearby biological fluids causing an apatite layer to precipitate on the implant surface. Titanium surfaces covered with calcium promote osteoblast cell adhesion, migration, and proliferation, as well as providing a roughened surface.⁹ Hydroxyapatite coatings on the surface of implants are frequently applied via plasma spraying,^{10–12} however, there are issues with this approach in terms of the coating thickness, purity and crystallinity, dissolution, adhesion, and fatigue failure.^{13,14}

Peri-implantitis and mucositis are the two most common inflammatory conditions leading to implant failure. They are mainly caused by bacterial colonization of the peri-implant site.^{15–17} The prevalence of mucositis has been noted in over 46% of subjects, while peri-implantitis has been noted in nearly 20% of subjects.¹⁸ The mechanical removal of adherent bacterial biofilm is essential to resolve the inflammatory condition when treating peri-implantitis,^{19,20} with optimal treatment aiming to detoxify and create a surface that can attract the osteoprogenitor cells in order to re-osseointegrate. In addition to its use to prepare new implant surfaces, blasting/air abrasion with abrasive powders is an effective mechanical method used to decontaminate infected implant surfaces to manage peri-implantitis.^{21–23} Several air abrasive mediums have been used with air abrasion, such as amino glycine powder and sodium bicarbonate.²⁴ HA can also be deposited onto titanium sur-

TABLE 1 Materials and surface modifications used in the study.

Material	Surface name	Surface treatment
CpTi 1	CpC	Control (No treatment)
	SB	Sandblasted with 250 μm Al_2O_3
	SBE	Sandblasted 250 μm Al_2O_3 /acid etched (3%HF/17.5% HNO_3)
CpTi 2	TiSLACT	Sandblasted 250–500 μm Al_2O_3 /acid etched ($\text{H}_2\text{SO}_4/\text{HCl}$)/rinsed with NaCl under N_2 /stored 0.9%NaCl
TiZr	RSLACT	Sandblasted 250–500 μm Al_2O_3 /acid etched ($\text{H}_2\text{SO}_4/\text{HCl}$)/rinsed with NaCl under N_2 /stored 0.9%NaCl

faces using air abrasion,^{25,26} but little research has been done on commercially available implants with existing surface modifications.^{12,25,26}

The aim of this study was to characterize the effect of airabrasion with bioceramic particles on commercially available implant surfaces. Previously prepared commercially available implant surfaces (CpTi) and a titanium-zirconia (TiZr) alloy were subjected to air abrasion for surface deposition using two novel bioceramic powder combinations (hydroxyapatite and calcium oxide). SEM and Energy Dispersive Spectroscopy (EDS) analysis were used to investigate the surface and elemental changes between the air-abraded specimens. The dissolution of the applied treatment from the surfaces over 3 weeks was also assessed.

MATERIALS AND METHODS

Three substrate implant materials from two companies were used in this study with different surfaces. Discs of relevant materials were obtained with surface modifications applied to the discs by the companies following the same methods used for the respective commercial products, as described below and summarized in Table 1.

1. Commercially pure titanium 1 grade 2 (Cp) ASTM F67 discs, 7 mm in diameter and 4 mm thick (S&S Biomat, Manchester, UK): Control (no treatment) (CpC). Sandblasted with 250 μm Al_2O_3 particles at 5 mm distance and a pressure of 8 bar, followed by ultrasonic cleaning for 20 min using an environmentally friendly detergent (15%–30% anionic surfactants, 5%–15% non-ionic surfactants), then washed with hot water and air pressure three times and dried in an oven (SB). Sandblasted as above, followed by acid etching in 3% hydrofluoric acid/17.5% nitric acid solution, followed by wash in distilled water and heat treatment at 200°C in an oven for 1 h (SBE).
2. Commercially pure titanium 2 grade 2 (Ti) discs (CpTi SLActive®), 5 mm in diameter and 1 mm thick (Institut Straumann AG, Basel, Switzerland). Sandblasted with

large grit 250–500 μm Al_2O_3 particles and acid etched with a boiling mixture of sulfuric/hydrochloric acids, then cleaned in nitric acid, rinsed in deionized water and air dried, followed by rinsing in NaCl solution under nitrogen treatment and storage in 0.9% NaCl solution (TiSLACT).

3. Titanium-zirconia alloy (13%–17% Zr) (R) (Roxolid®), discs 5 mm in diameter and 1 mm thick (Institut Straumann AG, Basel, Switzerland). Sandblasted with large grit 250–500 μm Al_2O_3 particles and acid etched with a boiling mixture of sulfuric/hydrochloric acids, then cleaned in nitric acid, rinsed in deionized water and air dried, followed by rinsing in NaCl solution under nitrogen treatment and storage in 0.9% NaCl solution (RSLACT). Discs of SLActive® and Roxolid® were received in plastic bottles filled with 0.9% NaCl, all other discs received were wrapped and sealed.

The powders were: (1) 95% hydroxyapatite (HA), $\text{Ca}_{10}(\text{PO}_4)_6(\text{OH})_2$ mixed with 5% calcium oxide (CaO) (MCD) (Hitemco Medical Applications, Inc., USA): 95% HA/5% CaO; (2) 90% hydroxyapatite (HA), $\text{Ca}_{10}(\text{PO}_4)_6(\text{OH})_2$ mixed with 10% calcium oxide (CaO) (MCD) (Hitemco Medical Applications, Inc., USA): 90% HA/10% CaO.

All discs were rinsed with deionized water and dried with an air dryer before air abrasion. Bioceramic powders were deposited by air abrasion onto the specimen. The PrepAir™ air abrasion unit (Danville, CA, USA) connected to an air compressor was used for air abrasion. In order to simulate the clinical situation, the distance between the spraying nozzle and the specimen was standardized to be 1–2 mm. The air abrasion was performed using a nozzle (tip size 0.48 mm \times 80°) at 0.41 MPa pressure, spraying time was standardized to be 2 min over the whole specimen. Pilot testing performed on different days, comparing different air abraded specimens using SEM confirmed the reproducibility of the technique.

Before the air abrasion process, the powders in this study were analyzed using Scanning electron microscopy and energy dispersive spectroscopy (SEM-EDS).

Surface roughness

The surface topography of the air-abraded discs was examined using an optical profilometer (Talysurf CLI 1000, Taylor Hobson Precision, UK). Surface measurements were obtained using the non-contacting confocal gauge measurement (CLA) gauge (300 μm) with the following specifications: 10 nm resolution at 30 mm/second speed. The resolution was optimized to obtain the best result at 1001 points/mm. All measurements were made over an area of 1 mm \times 1 mm with 1 μm spacing at a bidirectional speed. The Gaussian filter used was 0.8 mm with a 0.250 mm cut-off. Each disc was scanned three times over a randomly selected area. The scanned images were analyzed using Talymap Platinum software. The 3D surface roughness parameters assessed were S_a , S_p , and S_v , and their equivalent 2D parameters R_a , R_p , and R_v .

Scanning electron microscopy and energy dispersive spectroscopy (SEM-EDS)

An SEM (FEI Quanta 650 FEG) equipped with an energy dispersive spectroscopy (SEM-EDS, FEI Quanta 650 FEG, Oxford Instruments, UK) was used for surface structure and elemental analysis. Four specimens comprising one control (before treatment) and three treated specimens from each group per powder were examined and compared with SEM-EDS.

The treated specimens were mounted on aluminum stubs and loaded on the metal holder inside the SEM-EDS machine. The discs were assessed at different levels of magnification at an accelerated voltage of 20 kV and spot size of 3.5 nm, using both high and low vacuum modes. Elemental analysis was performed using EDS analysis software (Aztec Software, Ver.3.1). The specimens were mapped to determine the spread of the bioceramic treatment on the surfaces.

Inductively coupled plasma optical emission spectrometry (ICP-OES)

The ICP-OES (Perkin-Elmer Optima 5300 dual view, MA, USA) was used to assess the dissolution behavior of the bioceramic treatment. A pilot study was conducted where one specimen from each group (per powder) was placed in a glass tube and soaked in 50 mL of deionized water for 3 weeks. All specimens were then stored in an incubator at 37°C. A 10 mL specimen was taken from the test tubes at 1, 2, and 3 weeks. The concentrations of the Ca^{2+} and PO_4^{3-} released over the 3 weeks were assessed.

Sample size

For each group described above, six discs were used (total $n = 30$). For each group discs were treated with one of two apatite abrasive powders of sintered calcium phosphate (CaP, particle size: 53 μm), such that for each sub-group $n = 3$.

A sample size calculation (a priori) test was used to detect the minimum sample size needed for the study to achieve 80% power to detect a difference of 1.87. This is in line with similar studies using three specimens to evaluate the surface characteristics of implant surfaces between two independent groups of powders, considering a 5% significance level.^{27–31} In this study, nine measurements for each group per powder were evaluated.

Statistical analysis

A statistical software package (SPSS® Ver. 23, SPSS Inc., Chicago, IL) was used for the analysis. A test of normality revealed that data were not normally distributed and therefore data were assessed with a nonparametric test. A Kruskal-Wallis test with multiple pairwise comparisons was used to

TABLE 2 Elemental composition of the bioceramic powders.

Powder	O2 (%)	Ca (%)	P (%)	Ca/P ratio
95% HA/5% CaO	63.76	22.79	13.45	1.69
90% HA/10% CaO	78.14	15.59	6.26	2.49

compare the medians with the level of significance set to $p = 0.05$. For elemental data analysis, element weight percentages of (Ti, Ca, P) were recorded. The means and standard deviations from the four measurements for each specimen were calculated.

RESULTS

Powder analysis

The elemental composition of the bioceramic powders in atomic percentages showed that the two powders were mainly composed of O, Ca, and P, with some traces of Mg, Al, and Si (less than 1%) (Table 2).

Surface roughness

Different roughness parameters were recorded after treatment with different powders. For groups treated with 90% HA/10% CaO powders, there were no significant differences for all 2D and 3D roughness measurements across all groups (Figure 1).

The surface roughness medians and ranges for the specimens treated with 95% HA/5% CaO are summarized in Figure 1. The highest percentage of roughness change in Sa was recorded for TiSLACT 79.0% (SD 2.75), whereas the

lowest percentage of roughness change in Sa was recorded for the SB 11.8% (SD 2.38). The highest Sp was recorded for the CpC 58.03 μm (SD 5.90), whereas the lowest Sp was recorded for the RSLACT 16.53 μm (SD 2.22). For the Sv measurements, the TiSLACT group showed the highest value of 22.23 μm (SD 7.92), while the lowest Sv value of 9.97 μm (SD 1.78) was recorded for CpC. There was no statistically significant difference in the Sa, Sv, Ra, and Rv measurements across all material groups. The only statistically significant differences between the material groups were found in the Sp and Rp parameters ($p = 0.03$ and 0.04 , respectively). The pairwise comparisons for Sp revealed a statistically significant difference between CpC and SB, SBE, and RSLACT. CpC was also statistically different from the SBE for Rp. However, a comparison of the median differences in the average 3D roughness parameter Sa values before and after the bioceramic treatment (Table 3) did not show any significant differences with both powders ($p = 0.40$ and 0.40).

Scanning electron microscopy and energy dispersive spectroscopy analysis (SEM-EDS)

The micrographs acquired by SEM demonstrated that all specimens were covered with the bioceramic powders. A non-uniform distribution of the bioceramic powders was noted on the surface layer of all specimens (Figure 2). When comparing the surface structure of all discs before (Figure 2a) and after treatment (Figure 2b and c), it was clear that the bioceramic treatment created a different surface structure. Additionally, all discs had a similar surface with multiple grooves, rounded edges, and powder particles regardless of the material, surface modification, and the air abrasion powder used. Visible changes were noted in the control CpC

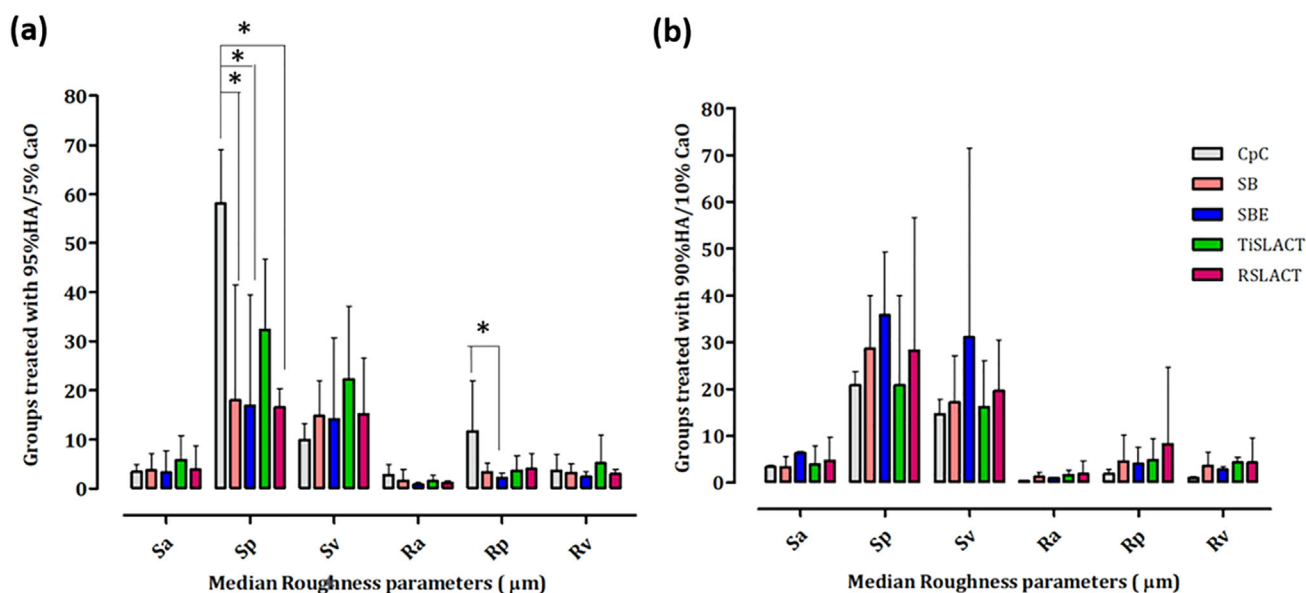


FIGURE 1 Bar charts representing the median roughness parameter for each group treated with 95% HA/5% CaO and 90% HA/10% CaO with error bars representing the range. The (*) represents a statistically significant difference.

TABLE 3 Medians of the S_a parameter and standard deviations (SD) with the percentage of roughness change for all groups before and after treatment with the bioceramic powders.

Group	Median S_a μm (SD)	Median S_a μm (SD)	Percentage of roughness change	Median S_a μm (SD)	Percentage of roughness change
	Before treatment	After treatment		After treatment	
CpC	3.00 (0.79)	3.45 (0.72)	15%	3.40 (0.17)	13.3%
SB	3.37 (0.11)	3.77 (1.87)	11.8%	3.35 (1.07)	0.6%
SBE	3.70 (1.53)	3.24 (2.38)	12.4%	6.30 (0.21)	70.2%
TiSLACT	3.24 (0.10)	5.80 (2.75)	79.0%	3.93 (2.06)	21.3%
RSLACT	2.56 (0.35)	3.89 (2.44)	51.9%	4.70 (2.62)	83.6%

group, where the surface changed from deep grooves to a surface with multiple depressions and projections.

The EDS analysis of the control specimens (no treatment) for CpC, SB, SBE, TiSLACT, and RSLACT showed the predominance of Ti and O as the main elements. Other trace elements were present at less than 1% (carbon, magnesium, aluminum, vanadium, and silicon) (Figure S9a). The elemental composition of the bioceramic powders showed that the two powders were mainly composed of O, Ca, and P, with some traces of Mg, Al, and Si (less than 1%).

Representative mapping of the bioceramic treatment distribution of each powder is presented in (Figures 3 and 4) with percentages of each atom (Figures S10 and 11). These images highlight the qualitative distribution of the elements within the specimens that were detected by the EDS analysis. From these maps, it can be observed that the Ca and P were detected and distributed all over the specimen, confirming that the powders were deposited on all surfaces. After applying the bioceramic treatment, Ca and P peaks appeared on the EDS spectrum as shown in the representative spectra (Figure S9b and c). Further images are provided in a supplementary folder. EDS elemental analysis of the specimens treated with 95% HA/5% CaO and 90% HA/10% CaO showed different median calcium and phosphate ratios on the surfaces. There were no significant differences in the Ca and P wt% between all groups and powders 95% HA/5% CaO and 90% HA/10% CaO ($p = 0.14$, 0.18 , and $p = 0.15$, 0.12 , respectively) (Table 4).

Inductively coupled plasma optic emission spectrometry (ICP-OES)

The concentrations of the Ca^{2+} and PO_4^{3+} released over the 3 weeks are plotted graphically in (Figure 5) and (Tables 5 and 6). Generally, the mean concentration of Ca^{2+} and PO_4^{3+} varied from week 1 to week 3. The pattern of Ca^{2+} release was different between the two powders (5% and 10% CaO). The pattern of Ca^{2+} for the 5% CaO powder in the first week (Figure 5a) was in the order of SBE 0.58 mg/L > SB 0.45 mg/L > CpC 0.43 mg/L > RSLACT 0.27 mg/L > TiSLACT 0.26 mg/L. A similar pattern was noted in the second and third weeks, except that the CpC group released more

TABLE 4 Medians and range of elemental (wt%) of calcium and phosphate with Ca/P ratios of all groups and powders.

	Specimens ($n = 3$)	Median Ca	Median P	Ca/P ratio
		wt% (range)	wt% (range)	
95% HA/ 5% CaO	CpC	24.50 (17.40)	7.99 (5.20)	3.06
	SB	8.33 (11.44)	2.51 (1.56)	3.31
	SBE	13.18 (4.65)	4.70 (1.61)	2.80
	TiSLACT	11.88 (8.20)	3.61 (3.23)	3.29
	RSLACT	8.45 (2.58)	2.41 (1.38)	3.50
90% HA/ 10% CaO	CpC	11.43 (13.74)	4.62 (4.86)	2.47
	SB	11.50 (6.69)	3.01 (4.05)	3.82
	SBE	14.65 (9.56)	6.15 (4.06)	2.38
	TiSLACT	7.90 (3.86)	3.18 (0.72)	2.48
	RSLACT	8.65 (4.59)	2.78 (1.76)	3.11

Ca^{2+} than the SB group. The pattern of Ca^{2+} released from the 10% CaO powder was different from the 5% CaO powder. The order of Ca^{2+} release over the 3-week period was CP > TiSLACT > SBE > RSLACT > SB (Figure 5b).

DISCUSSION

The use of air abrasion with a bioceramic abrasive to modify the implant surface properties and introduce a surface that might favor re-osseointegration was evaluated in this study. No previous studies have been reported using air abrasion on implant surfaces with the combinations of bioceramic powders in this study (hydroxyapatite and calcium oxide). Furthermore, the influence of such treatment on surface properties and dissolution behavior has not been assessed to date.

Previous research has demonstrated that varying air abrasive powder parameters, including the powder formulation and particle size, might influence the surface characteristics.^{32,33} The addition of CaO to HA powders results in different Ca/P ratios correlated to the dissolution rate of CaP coatings;³⁴ hence why two formulations of bioceramic powders were chosen. Previous studies using similar

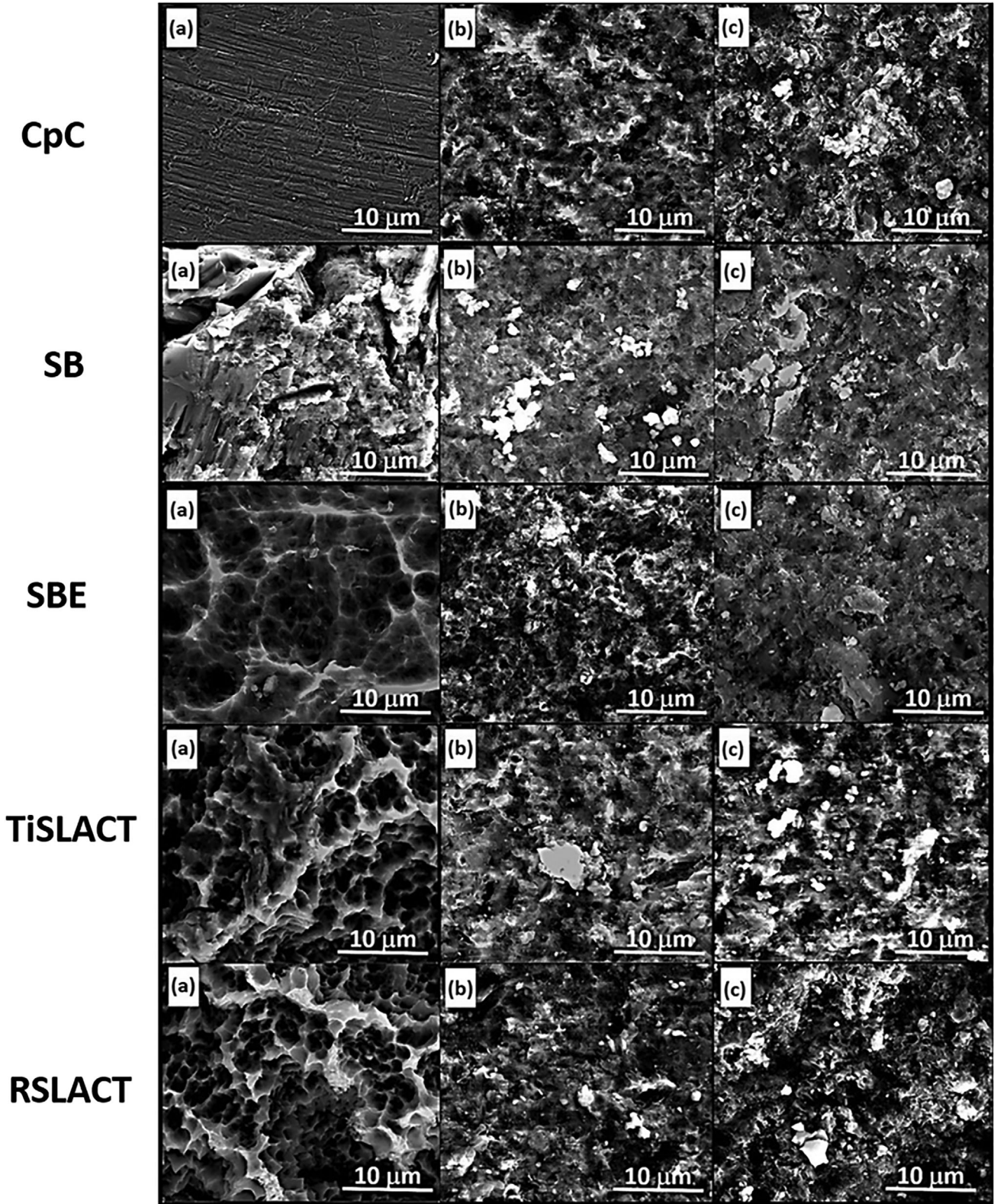


FIGURE 2 Representative SEM images at 5,000x magnification of all tested specimens showing the change in surface structure; CpC, SB, SBE, TiSLACT (SLActive®) and RSLACT (Roxolid®), (a) without treatment, (b) treated with 95% HA/5% CaO, and (c) treated with 90% HA/10% CaO.

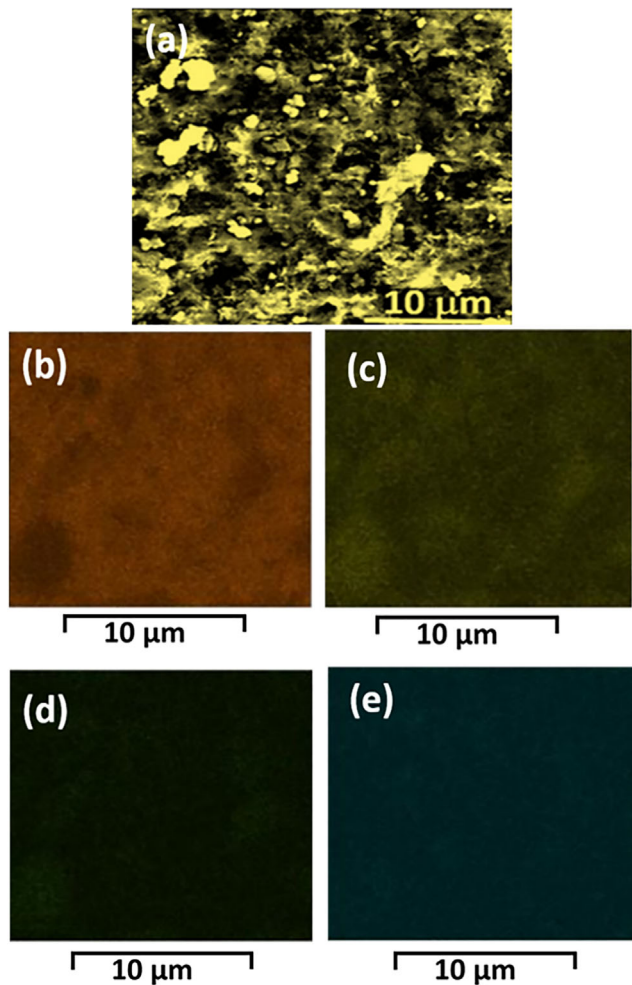


FIGURE 3 Representative map of the bioceramic elemental distribution on the TiSLACT surface treated with 90% HA/10% CaO: (a) representing the layered SEM image, (b) titanium, (c) calcium, (d) phosphate, (e) oxygen.

bioceramic powders have not specified the exact formulas used.^{35–37} In our study the composition was systematically set at 5% and 10% CaO in order to examine the effect of CaO concentration on the properties studied.

The SEM and EDS surface analyses demonstrated the incorporation of abrasive powders on the treated surfaces. The material substrate and existing surface modification had no significant effect on the change in surface characteristics when using the 90% HA/10% CaO, whereas with the 95% HA/5% CaO powder the material substrate and existing surface had a significant effect on the Sp and Rp parameters only. This significant effect on Sp and Rp could be related to the different powder compositions used. Although the specimens had different microstructures before treatment and after treatment, the morphological appearance of all air-abraded specimens regardless of the material and existing surface appeared similar: all were rough and irregular with several depressions and projections observed across the surface.

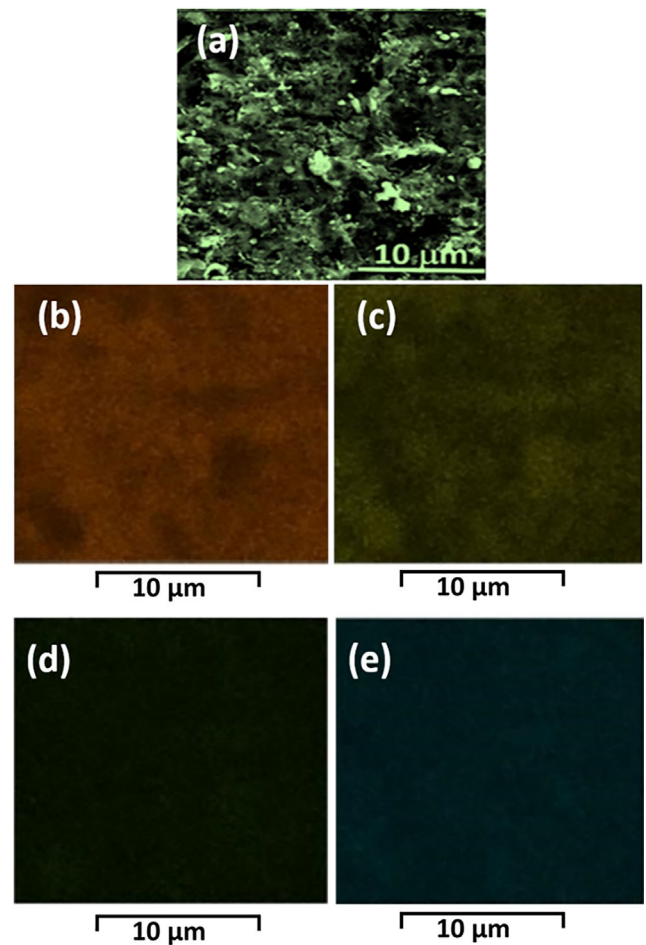


FIGURE 4 Representative map of the bioceramic elemental distribution on the RSLACT surface treated with 95% HA/5% CaO: (a) representing the layered SEM image, (b) titanium, (c) calcium, (d) phosphate, (e) oxygen.

To date, limited studies have used air abrasion to deposit bioceramic abrasive powders on surface-modified CpTi, with no studies using the method employed in this study or bioceramic powders on TiZr alloy with different surfaces.^{8,25,26} The Sa values post-treatment varied to pre-treatment, however, when statistically comparing the Sa parameter no significant differences were noted between the before and after treatment for both powders. This could be explained by the non-uniformity of the coating on the surface, where some areas might have more particles than others, and different powder compositions might also have produced different effects on the surface. When comparing the 3D views of the bioceramic treated specimens and the untreated specimens the change in surface topography was presented as projections that most likely represent the deposited bioceramic powders on the surfaces, as confirmed by the EDS analysis.

The qualitative SEM images confirmed that the bioceramic treatment changed the surface morphology of the tested specimens, in agreement with other studies using air abrasion.^{26,38} However, the surface morphology of all treated surfaces

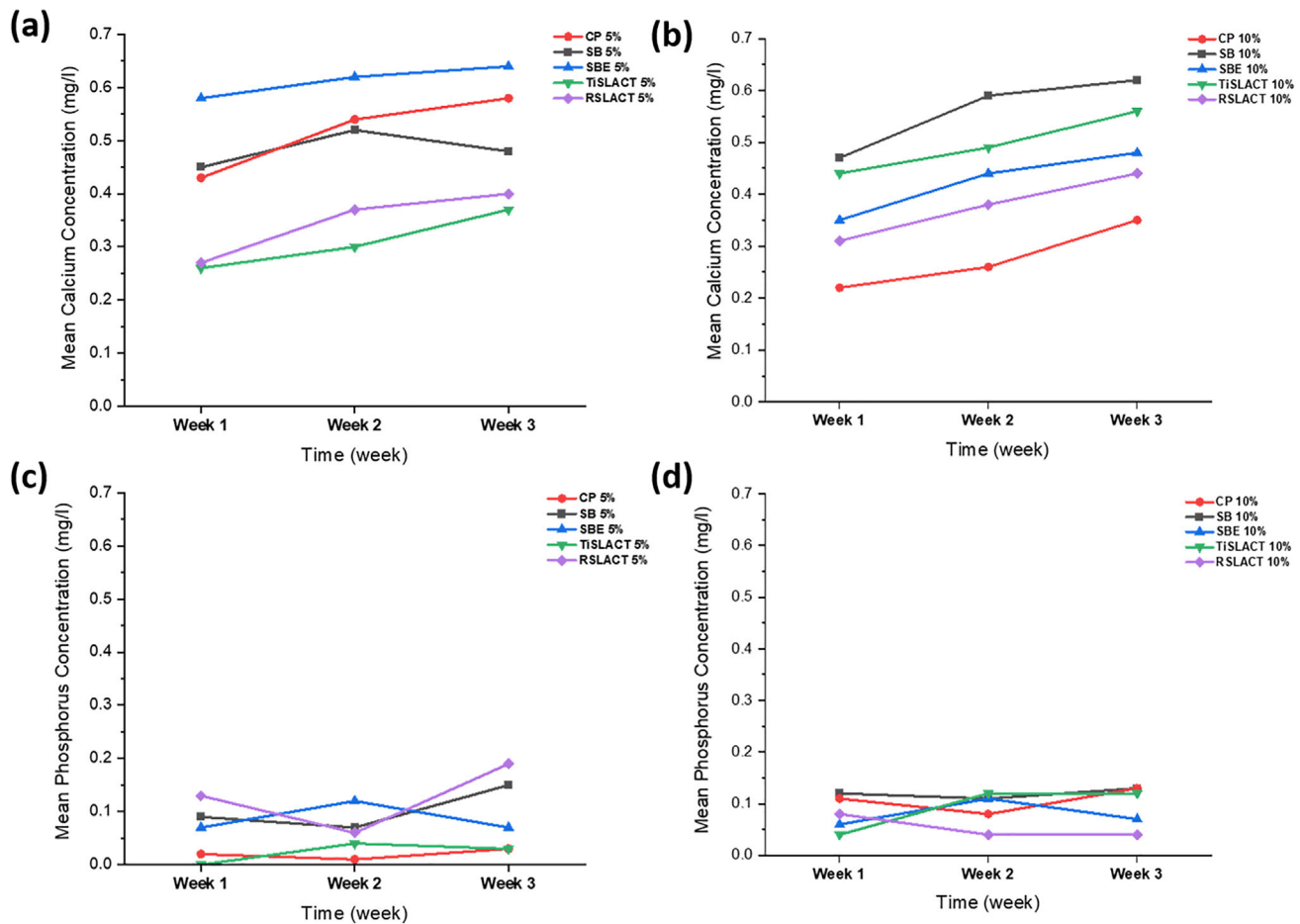


FIGURE 5 Mean calcium ion release and standard deviation for the specimens treated with (a) 95% HA/5% CaO, (b) 90% HA/10% CaO over 3 weeks. The mean phosphorous ion release and standard deviation for the specimens treated with (c) 95% HA/5% CaO, (d) 90% HA/10% CaO over 3 weeks.

revealed a non-uniform distribution of the treatment on the surface layer of the specimens, with dispersed patches of bio-ceramic powders spread over the surface. This was confirmed by the EDS analysis that demonstrated Ca/P-rich surfaces at different concentrations from the same specimen and is in agreement with other studies using air abrasion with bio-ceramic abrasives.^{23,39} The EDS analysis of the treated surfaces also showed the peaks of titanium in all the resulting spectrums, which means that the effect of the treatment was limited to the surface layer of the specimens. The weight percentages of Ca and P varied with no statistically significant differences, this could be attributed to the different surfaces or the different concentrations of the powders. The CpC surface, which was not exposed to any surface modification before the bio-ceramic treatment showed a high wt% of both Ca and P for both powders, which may be due to its surface being anisotropic and having deep grooves.⁴⁰ However, it did not show any significant difference to the other tested groups in relation to the Ca/P ratios with both powder compositions.

The dissolution (and rate) of Ca^{2+} and PO_4^{3+} from HA bioceramics is crucial to stimulate the osseointegrative characteristics of the implant surface during tissue healing. Assessment of coating dissolution has been evaluated

by immersing coated specimens in liquid solutions such as simulated body fluid (SBF), deionized water, Ringer's solutions, and distilled water.^{41,42} In this study, similar to previous research,⁴³ deionized water was used as immersing media to avoid any possible interference that may result from different electrolytes in the immersion media. Due to its sensitivity and accuracy, inductively coupled plasma optical emission spectrometry (ICP-OES) is one of the most extensively used methods to detect trace elements released from treated titanium surfaces.^{36,44}

The concentrations of Ca^{2+} and PO_4^{3+} released varied, with heterogeneity between the specimens. In general, the amount of Ca^{2+} released over the 3 weeks was higher than the PO_4^{3+} released. This could be due to the different concentrations of CaO added to the bio-ceramic powders by the company (i.e., the Ca^{2+} released could be from the HA and the extra CaO, where the PO_4^{3+} originates from the HA component only).

CaP-based bioceramics applied by air abrasion have been suggested to enhance cell viability at 6 days post-treatment.³⁹ Therefore, the dissolution of the bio-ceramic abrasives in the present study for 3 weeks should enhance the cellular response and subsequent implant bioactivity. The Ca^{2+} and

TABLE 5 Representing the mean calcium ion released (SD) for the specimens treated with 95% HA/5% CaO, and 90% HA/10% CaO over 3 weeks.

Sample	Mean Ca mg/L week 1 (SD)	Mean Ca mg/L week 2 (SD)	Mean Ca mg/L week 3 (SD)
SB 5%	0.45 (0.08)	0.52 (0.08)	0.48 (0.05)
SB 10%	0.22 (0.06)	0.26 (0.06)	0.35 (0.07)
CP 5%	0.43 (0.06)	0.54 (0.06)	0.58 (0.06)
CP 10%	0.47 (0.08)	0.59 (0.08)	0.62 (0.11)
SBE 5%	0.58 (0.05)	0.62 (0.05)	0.64 (0.07)
SBE 10%	0.35 (0.06)	0.44 (0.06)	0.48 (0.06)
TiSLACT 5%	0.26 (0.04)	0.30 (0.05)	0.37 (0.06)
TiSLACT 10%	0.44 (0.08)	0.49 (0.05)	0.56 (0.08)
RSLACT 5%	0.27 (0.06)	0.37 (0.05)	0.40 (0.07)
RSLACT 10%	0.31 (0.04)	0.38 (0.08)	0.44 (0.07)

TABLE 6 Representing the mean phosphorous ion released (SD) for the specimens treated with 95% HA/5% CaO, and 90% HA/10% CaO over 3 weeks.

Sample	Mean P mg/L week 1 (SD)	Mean P mg/L week 2 (SD)	Mean P mg/L week 3 (SD)
SB 5%	0.02 (0.10)	0.01 (0.05)	0.03 (0.11)
SB 10%	0.11 (0.08)	0.08 (0.02)	0.13 (0.11)
CP 5%	0.09 (0.04)	0.07 (0.04)	0.15 (0.10)
CP 10%	0.12 (0.03)	0.11 (0.04)	0.13 (0.08)
SBE 5%	0.07 (0.05)	0.12 (0.09)	0.07 (0.04)
SBE 10%	0.06 (0.05)	0.11 (0.03)	0.07 (0.03)
TiSLACT 5%	0.00 (0.09)	0.04 (0.02)	0.03 (0.02)
TiSLACT 10%	0.04 (0.10)	0.12 (0.10)	0.12 (0.02)
RSLACT 5%	0.13 (0.12)	0.06 (0.04)	0.19 (0.01)
RSLACT 10%	0.08 (0.07)	0.04 (0.04)	0.04 (0.06)


PO₄³⁺ may continue to be released from the thin coating on the treated surfaces after 3 weeks, although any such sustained release is unlikely to have any negative effect on the healing process, unlike the previously used thick HA coatings which were prone to failure.⁴⁵ The slow dissolution rate of the bioceramic treatment in this study could be related to the crystallinity of the HA powder, with crystalline coatings having been shown to dissolve slower in vivo and in vitro.^{46,47} Further characterization of implant surfaces and in vivo studies are needed to assess if these deposits will stimulate a beneficial cellular response during tissue healing.

In conclusion, air abrasion embedded bioceramic abrasive particles on CpTi and TiZr surfaces leaving powder deposits, with a minimal change in surface characteristics. Varying the powder composition might affect the resulting surface characteristics. Dissolution of Ca²⁺ and PO₄³⁺ from the bioceramic-treated specimens confirmed the stability and the continuous release of the bioceramic treatment over 3 weeks.

CONFLICT OF INTEREST STATEMENT

We have no conflict of interest to declare.

ORCID

Nesreen A. Salim BDS, MSc, PhD  <https://orcid.org/0000-0002-5355-2269>

Lamyia M. Anweigi BDS, MMedSc, MFDS, PhD  <https://orcid.org/0000-0002-5632-0471>

REFERENCES

- Jivraj S, Chee W. Rationale for dental implants. *Br Dent J*. 2006;200:661-65
- Griggs JA. Dental implants. *Dent Clin North Am*. 2017;61:857-71
- Elani HW, Starr JR, Da Silva JD, Gallucci GO. Trends in Dental Implant Use in the U.S., 1999–2016, and Projections to 2026. *J Dent Res*. 2018;97:1424-30
- Albrektsson T, Zarb GA. Current interpretations of the osseointegrated response: clinical significance. *Int J Prosthodont*. 1993;6:95-105
- Ballo AM, Omar O, Xia W, Palmquist A. Dental implant surfaces-Physicochemical properties, biological performance, and trends. *Implant Dentistry-A Rapidly Evolving Practice*;1:19-56
- Rutkowski JL: Fundamentals of implant dentistry: prosthodontic principles. Beumer J III, Faulkner RF, Shah KC, Moy PK. Hanover Park, Ill: Quintessence Publishing, 2015. *J Oral Implantol*. 2015;41:343
- Anitua E, Piñas L, Murias A, Prado R, Tejero R. Effects of calcium ions on titanium surfaces for bone regeneration. *Colloids Surf B Biointerfaces*. 2015;130:173-81
- Cooper LF. A role for surface topography in creating and maintaining bone at titanium endosseous implants. *J Prosthet Dent*. 2000;84:522-34
- Legeros RZ. Properties of osteoconductive biomaterials: calcium phosphates. *Clin Orthop Relat Res*. 2002;395: 81-98
- Tsui YC, Doyle C, Clyne TW. Plasma sprayed hydroxyapatite coatings on titanium substrates. Part 1: mechanical properties and residual stress levels. *Biomaterials*. 1998;19:2015-29
- Huang HH, Chen JY, Lin MC, Wang YT, Lee TL, Chen L-K. Blood responses to titanium surface with TiO₂ nano-mesh structure. *Clin Oral Implants Res*. 2012;23:379-83
- Chopra D, Jayasree A, Guo T, Gulati K, Ivanovskiet S. Advancing dental implants: bioactive and therapeutic modifications of zirconia. *Bioact Mater*. 2022;13:161-78
- Toque JA, Herliansyah MK, Hamdi M, Ide-Ektessabi A, Sopyan I. Adhesion failure behavior of sputtered calcium phosphate thin film coatings evaluated using microscratch testing. *J Mech Behav Biomed Mater*. 2010;3:324-30
- Sun L, Berndt CC, Gross KA, Kucuk A. Material fundamentals and clinical performance of plasma-sprayed hydroxyapatite coatings: a review. *J Biomed Mater Res*. 2001;58:570-92
- Pérez-Chaparro PJ, Duarte PM, Shibli JA, Montenegro S, Lacerda Heluy S, Figueiredo LC, et al. The current weight of evidence of the microbiologic profile associated with peri-implantitis: a systematic review. *J Periodontol*. 2016;87:1295-304
- Derks J, Tomasi C. Peri-implant health and disease. A systematic review of current epidemiology. *J Clin Periodontol*. 2015;42 Suppl 16:S158-71
- Salvi GE, Cosgarea R, Sculean A. Prevalence and mechanisms of peri-implant diseases. *J Dent Res*. 2017;96:31-37
- Lee CT, Huang YW, Zhu L, Weltman R. Prevalences of peri-implantitis and peri-implant mucositis: systematic review and meta-analysis. *J Dent*. 2017;62:1-12
- Smeets R, Henningsen A, Jung O, Heiland M, Hammächer C, Stein JM. Definition, etiology, prevention and treatment of peri-implantitis – a review. *Head Face Med*. 2014;10:34
- Suarez F, Monje A, Galindo-Moreno P, Wang HL. Implant surface detoxification: a comprehensive review. *Implant Dent*. 2013;22:465-73
- Ronay V, Merlini A, Attin T, Schmidlin PR, Sahrman P. In vitro cleaning potential of three implant debridement methods.

- Simulation of the non-surgical approach. *Clin Oral Implants Res.* 2017;28:151-55
22. Schwarz F, Becker K, Renvert S. Efficacy of air polishing for the non-surgical treatment of peri-implant diseases: a systematic review. *J Clin Periodontol.* 2015;42:951-59
 23. Tastepe CS, van Waas R, Liu Y, Wismeijer D. Air powder abrasive treatment as an implant surface cleaning method: a literature review. *Int J Oral Maxillofac Implants.* 2012;27:1461-73
 24. Sahm N, Becker J, Santel T, Schwarz F. Non-surgical treatment of peri-implantitis using an air-abrasive device or mechanical debridement and local application of chlorhexidine: a prospective, randomized, controlled clinical study. *J Clin Periodontol.* 2011;38:872-78
 25. Kulkarni Aranya A, Pushalkar S, Zhao M, Legeros RZ, Zhang Y, Saxena D. Antibacterial and bioactive coatings on titanium implant surfaces. *J Biomed Mater Res A.* 2017;105:2218-27
 26. Koller G, Cook RJ, Thompson ID, Watson TF, Di Silvio L. Surface modification of titanium implants using bioactive glasses with air abrasion technologies. *J Mater Sci Mater Med.* 2007;18:2291-96
 27. Coelho PG, Lemons JE. Physico/chemical characterization and in vivo evaluation of nanothickness bioceramic depositions on alumina-blasted/acid-etched Ti-6Al-4 V implant surfaces. *J Biomed Mater Res A.* 2009;90A:351-61
 28. Lotz EM, Olivares-Navarrete R, Hyzy SL, Berner S, Schwartz Z, Boyan BD. Comparable responses of osteoblast lineage cells to microstructured hydrophilic titanium-zirconium and microstructured hydrophilic titanium. *Clin Oral Implants Res.* 2017;28:e51-e59
 29. Hakki SS, Tatar G, Dundar N, Demiralp B. The effect of different cleaning methods on the surface and temperature of failed titanium implants: an in vitro study. *Lasers Med Sci.* 2017;32:563-71
 30. John G, Becker J, Schwarz F. Effectivity of air-abrasive powder based on glycine and tricalcium phosphate in removal of initial biofilm on titanium and zirconium oxide surfaces in an ex vivo model. *Clin Oral Investig.* 2016;20:711-19
 31. Rupp F, Scheideler L, Olshanska N, De Wild M, Wieland M, Geis-Gerstorfer J. Enhancing surface free energy and hydrophilicity through chemical modification of microstructured titanium implant surfaces. *J Biomed Mater Res A.* 2006;76A:323-34
 32. Schwarz F, Ferrari D, Popovski K, Hartig B, Becker J. Influence of different air-abrasive powders on cell viability at biologically contaminated titanium dental implants surfaces. *J Biomed Mater Res B Appl Biomater.* 2009;88B:83-91
 33. Menini M, Piccardo P, Baldi D, Dellepiane E, Pera P. Morphological and chemical characteristics of different titanium surfaces treated by bicarbonate and glycine powder air abrasive systems. *Implant Dent.* 2015;24:47-56
 34. Hwang JW, Lee EU, Lee JS, Jung UW, Lee IS, Choi S-H. Dissolution behavior and early bone apposition of calcium phosphate-coated machined implants. *J Periodontal Implant Sci.* 2013;43:291-300
 35. Ahn S, Vang MS, Yang HS, Park SW, Lim HP. Histologic evaluation and removal torque analysis of nano- and microtreated titanium implants in the dogs. *J Adv Prosthodont.* 2009;1:75-84
 36. O'Sullivan C, O'Hare P, Byrne G, O'Neill L, Ryan KB, Crean AM. A modified surface on titanium deposited by a blasting process. *Coatings.* 2011;1:53-71
 37. Barry JN, Twomey B, Cowley A, O'neill L, McNally PJ, Dowling DP. Evaluation and comparison of hydroxyapatite coatings deposited using both thermal and non-thermal techniques. *Surf Coat Technol.* 2013;226:82-91
 38. Duarte PM, Reis AF, De Freitas PM, Ota-Tsuzuki C. Bacterial adhesion on smooth and rough titanium surfaces after treatment with different instruments. *J Periodontol.* 2009;80:1824-32
 39. Tastepe CS, Lin X, Werner A, Donnet M, Wismeijer D, Liu Y, et al. Cleaning effect of osteoconductive powder abrasive treatment on explanted human implants and biofilm-coated titanium discs. *Clin Exp Dent Res.* 2018;4:25-34
 40. Elias C, Oshida Y, Lima J, Muller C. Relationship between surface properties (roughness, wettability and morphology) of titanium and dental implant removal torque. *J Mech Behav Biomed Mater.* 2008;1:234-42
 41. Gu YW, Khor KA, Cheang P. In vitro studies of plasma-sprayed hydroxyapatite/Ti-6Al-4 V composite coatings in simulated body fluid (SBF). *Biomaterials.* 2003;24:1603-11
 42. Wang H, Eliaz N, Xiang Z, Hsu HP, Spector M, Hobbs LW. Early bone apposition in vivo on plasma-sprayed and electrochemically deposited hydroxyapatite coatings on titanium alloy. *Biomaterials.* 2006;27:4192-203
 43. Kim H, Choi SH, Chung SM, Li LH, Lee IS. Enhanced bone forming ability of SLA-treated Ti coated with a calcium phosphate thin film formed by e-beam evaporation. *Biomed Mater.* 2010;5:044106
 44. Hung KY, Lin YC, Feng HP. The effects of acid etching on the nanomorphological surface characteristics and activation energy of titanium medical materials. *Materials (Basel).* 2017;10:1164.
 45. Artzi Z, Carmeli G, Kozlovsky A. A distinguishable observation between survival and success rate outcome of hydroxyapatite-coated implants in 5–10 years in function. *Clin Oral Implants Res.* 2006;17:85-93.
 46. Dunne CF, Gibbons J, Fitzpatrick DP, Mulhall KJ, Stanton KT. On the fate of particles liberated from hydroxyapatite coatings in vivo. *Ir J Med Sci.* 2015;184:125-33.
 47. Dunne CF, Twomey B, O'Neill L, Stanton KT. Co-blasting of titanium surfaces with an abrasive and hydroxyapatite to produce bioactive coatings: substrate and coating characterisation. *J Biomater Appl.* 2014;28:767-78.

SUPPORTING INFORMATION

Additional supporting information can be found online in the Supporting Information section at the end of this article.

How to cite this article: Abuhajar E, Salim NA, Satterthwaite JD, Silikas N, Anweigi LM. Effect of bioceramic powder abrasion on different implant surfaces. *J Prosthodont.* 2024;1–10.
<https://doi.org/10.1111/jopr.13857>